Structure and X-ray powder reference patterns for hexagonal perovskite-related phases, $(Sr_{0.8}Ca_{0.2})_5Co_4O_{12}$ and $Sr_6Co_5O_{15}$

W. Wong-Ng[a)]
Ceramics Division, National Institute of Standards and Technology, Gaithersburg, Maryland 20899

J. A. Kaduk
Poly Crystallography, Inc., Naperville, Illinois 60540

G. Liu
Ceramics Division, National Institute of Standards and Technology, Gaithersburg, Maryland 20899

(Received 17 November 2010; accepted 16 January 2011)

Two selected members of the homologous series $A_{n+2}BB'_nO_{3n+3}$ (A=Sr and Ca; B and B'=Co) have been investigated for their crystal structures because of their potential applications as thermoelectric materials. A combined Rietveld refinement and spin-polarized magnetic geometry optimization technique was employed for the structural studies. Both the n=3 member, $(Sr_{0.8}Ca_{0.2})_5Co_4O_{12}$, and the n=4 member, $Sr_6Co_5O_{15}$, have distorted hexagonal perovskite-related structures that possess one-dimensional cobalt oxide chains separated by alkaline-earth cations. The linear chains consist of one unit of CoO_6 trigonal prism alternating with n units of CoO_6 octahedra. Crystal structures and reference powder X-ray diffraction patterns of $(Sr_{0.8}Ca_{0.2})_5Co_4O_{11}$ [$P3c1$, a=9.4196(2) Å, c=19.9857(6) Å, V=825.83 Å^3, and D_x=5.358 g/cm^3] and $Sr_6Co_5O_{15}$ [$R32$, a=9.497 64(12) Å, c=12.3956(2) Å, V=968.34 Å^3, and D_x=5.455 g/cm^3] are reported. © *2011 International Centre for Diffraction Data.* [DOI: 10.1154/1.3555294]

Key words: thermoelectric materials, $A_{n+2}BB_{n'}O_{3n+3}$ homologous series, $(Sr_{0.8}Ca_{0.2})_5Co_4O_{12}$, $Sr_6Co_5O_{15}$, crystal structure, reference patterns

I. INTRODUCTION

The efficiency and performance of thermoelectric materials for power generation or cooling applications is related to the dimensionless figure of merit (ZT), given by

$$ZT = S^2\sigma T/k, \quad (1)$$

where T is the absolute temperature, S is the Seebeck coefficient or thermopower, σ is the electrical conductivity ($\sigma = 1/\rho$, whereρ is the electrical resistivity), and k is the thermal conductivity (Tritt, 1996; Tritt and Subramanian, 2006). Until recently, only a small number of materials were found to have practical industrial applications. Increased research and development of thermoelectric materials has been mostly driven by the need for more efficient energy utilization and the dramatic increase in ZT values of materials recently discovered (Hsu *et al.*, 2004; Venkatasubramanian *et al.*, 2001; Ghamaty and Eisner, 1999; Dresselhaus *et al.*, 2007; Funahashi *et al.*, 2004).

Novel thermoelectric oxides that were discovered within the past decade have been of great interest to the thermoelectric community for high-temperature applications. For example, low dimensional cobaltites $NaCoO_x$ (Terasaki *et al.*, 1997), $Ca_2Co_3O_6$ (Mikami and Funahashi, 2005; Mikami *et al.*, 2003), and $Ca_3Co_4O_9$ (Grebille *et al.*, 2004; Masset *et al.* 2000; Minami *et al.*, 2002) exhibit coexistence of large thermopower and low electrical resistivity. These compounds also have high electronic anisotropy. In $NaCoO_x$ and $Ca_3Co_4O_9$ (Terasaki *et al.*, 1997; Grebille *et al.*, 2004; Masset *et al.* 2000; Minami *et al.*, 2002), the presence of Co-O layers appears to be critical for contributing to the desirable properties. The $Ca_3Co_4O_9$ phase has the best thermoelectric property among the known oxides due to its distinctive misfit-layered oxide structure that features two penetrating incommensurate lattices with common a and c, and β parameters but with different b (Masset *et al.*, 2000). These misfit layers were thought to scatter phonons, thereby lowering the thermal conductivity. Subsequent to these discoveries, studies of low dimensional cobaltites, including materials with dopants either on Ca or Co sites, have been increasing.

We have previously reported the phase diagram and thermoelectric properties of selected members in the Sr-Ca-Co-O system (Wong-Ng *et al.*, 2010). In this system, in addition to the reported $(Ca,Sr)_3Co_4O_9$ phase, there are two homologous series of compounds, $(Ca,Sr)_{n+2}Co'Co_nO_{3n+3}$ and $(Sr,Ca)_{n+2}Co'Co_nO_{3n+3}$. While the members of the $Ca_{n+2}Co_nCo'O_{3n+3}$ and $Sr_{n+2}Co_nCo'O_{3n+3}$ series have reasonably high Seebeck coefficients and relatively low thermal conductivity, the electrical conductivity needs to be increased in order to achieve high ZT values. Although we have determined their solid solution limits for the $Ca_{n+2}Co_nCo'O_{3n+3}$ and $Sr_{n+2}Co_nCo'O_{3n+3}$ series, the structures of the n=3 ($Sr_5Co_4O_{12}$) and n=4 ($Sr_6Co_5O_{15}$) members have not been determined definitively. For example, only an ideal structure of $Sr_5Co_4O_{12}$ has been derived from high-resolution electron microscopy (Christoffersen *et al.*, 1997; Boulahya *et al.*, 1999a). Structures of related phases such as $Ba_5CuIr_3O_{12}$ and $(Sr_{0.75}Ba_{0.25})_5NiMn_3O_{12}$ have been determined to have space groups $P321$ (Blake *et al.*, 1999) and P-3$c1$ (Hernando *et al.*, 2003), respectively. It has also been reported that $Sr_5Co_4O_{12}$ is isostructural with $Sr_5Ni_4O_{11}$ (Lee and Holland, 1991). However, a later report by Abraham *et al.* (1994) indicated that $Sr_5Ni_4O_{11}$ was actually a mixed-valence com-

[a)]Author to whom correspondence should be addressed. Electronic mail: winnie.wong-ng@nist.gov

TABLE I. Rietveld refinement results of $(Sr_{0.8}Ca_{0.2})_5Co_4O_x$. The R_{wp} and R_p values are calculated including the background.

R_{wp}	0.0824
R_p	0.0607
χ^2	2.894
Percentage from restraints	31.6
No. of observations	10579
No. of variables	42
$R(F)$	0.0661
$R(F^2)$	0.0875
Normal probability plot, slope	1.1461
intercept	0.0442
ΔF, eÅ^{-3}, +	4.9 (near Sr3/Ca3)
	4.1 (near Sr2/Ca2)
...	−2.1

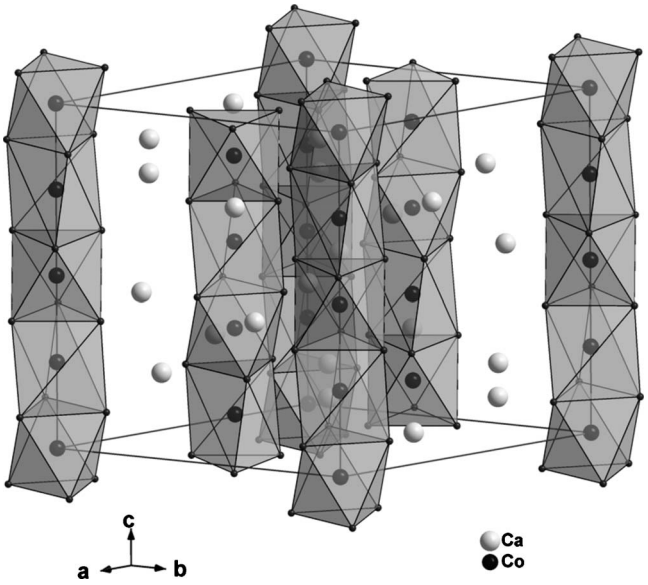

Figure 1. The structure of the homologous series of compounds, $A_{n+2}Co_nCo'O_{3n+3}$ (A=alkali earth elements), with n=1 (Wong-Ng *et al.*, 2010; Boulahya *et al.*, 1999a; Boulahya *et al.*, 1999b).

pound of formula $Sr_4Ni_3O_9$. For the structure of $Sr_6Co_5O_{15}$, there exist two conflicting reported space groups of $R32$ (Harrison *et al.*, 1995; Iwasaki *et al.*, 2003, 2006; Rodriguez *et al.*, 1987) and $R\bar{3}$ (Sun *et al.*, 2006).

The first goal of this paper is to clarify the structure of the n=3 and n=4 members in the $(Sr,Ca)_{n+2}Co'Co_nO_{3n+3}$ series by determining the structure of $(Sr_{0.8}Ca_{0.2})_5Co_4O_{11}$ and $Sr_6Co_5O_{15}$ using the combined X-ray Rietveld refinement with a spin-polarized magnetic geometry optimization technique. Currently, the Powder Diffraction File (PDF) of International Centre for Diffraction Data (ICDD) only contains calculated patterns for $Sr_5Co_4O_{12}$ (PDF 04-011-1857) (ICDD, 2010) and for $Sr_6Co_5O_{15}$ (PDF 01-075-3227, 04-

TABLE II. Atomic coordinates of atoms in $(Sr_{0.8}Ca_{0.2})_5Co_4O_{12}$, $P\bar{3}c1$. The atomic coordinates for the oxygen ions were obtained from quantum mechanical calculations.

Atom	X	Y	Z	Occupancy	U_{iso}	Site
Sr1/Ca1	0.6442(30)	−0.0035(32)	−0.0080(13)	0.75/0.25(8)	0.0081(5)	6*d*
Sr2/Ca2	0.3260(34)	−0.0124(23)	0.0936(13)	0.85/0.15(7)	0.0081(5)	6*d*
Sr3/Ca3	0.6618(19)	−0.0282(18)	0.2013(9)	0.86/0.14(7)	0.0081(5)	6*d*
Sr4/Ca4	0.3322(24)	0.0146(23)	0.2949(9)	0.86/0.14(10)	0.0081(5)	6*d*
Sr5/Ca5	0.6911(20)	0.0244(20)	0.4004(14)	0.78/0.22(6)	0.0081(5)	6*d*
Co1	0.0	0.0	−0.0072(6)	1.0	0.0023(11)	2*a*
Co2	0.0	0.0	0.2429(6)	1.0	0.0023(11)	2*a*
Co3	0.0	0.0	0.1236(6)	1.0	0.0023(11)	2*a*
Co4	0.0	0.0	0.3636(6)	1.0	0.0023(11)	2*a*
Co5	0.333 33	0.666 67	0.4013(6)	1.0	0.0023(11)	2*b*
Co6	0.333 33	0.666 67	0.5302(6)	1.0	0.0023(11)	2*b*
Co7	0.333 33	0.666 67	0.1511(6)	1.0	0.0023(11)	2*b*
Co8	0.333 33	0.666 67	0.2710(6)	1.0	0.0023(11)	2*b*
Co9	0.666 67	0.333 33	0.1971(6)	1.0	0.0023(11)	2*c*
Co10	0.666 67	0.333 33	0.3257(6)	1.0	0.0023(11)	2*c*
Co11	0.666 67	0.333 33	0.0682(6)	1.0	0.013(12)	2*c*
Co12	0.666 67	0.333 33	0.4474(6)	1.0	0.0023(11)	2*c*
O1	0.497 07	0.187 28	0.006 69	1.0	0.011 33	6*d*
O2	0.188 56	0.506 21	−0.030 69	1.0	0.011 33	6*d*
O3	0.154 18	0.145 37	0.061 96	1.0	0.011 33	6*d*
O4	0.617 36	0.165 49	0.131 17	1.0	0.011 33	6*d*
O5	0.336 14	0.511 16	0.090 96	1.0	0.011 33	6*d*
O6	0.160 78	0.005 21	0.1848	1.0	0.011 33	6*d*
O7	0.1737	0.510 23	0.209 13	1.0	0.011 33	6*d*
O8	0.157 49	0.156 65	0.302 89	1.0	0.011 33	6*d*
O9	0.713 61	0.212 87	0.263 37	1.0	0.011 33	6*d*
O10	0.346 59	0.5239	0.332 17	1.0	0.011 33	6*d*
O11	0.145 56	−0.013 82	0.424 62	1.0	0.011 33	6*d*
O12	0.520 38	0.1641	0.387 55	1.0	0.011 33	6*d*

https://doi.org/10.1154/1.3555294 Published online by Cambridge University Press

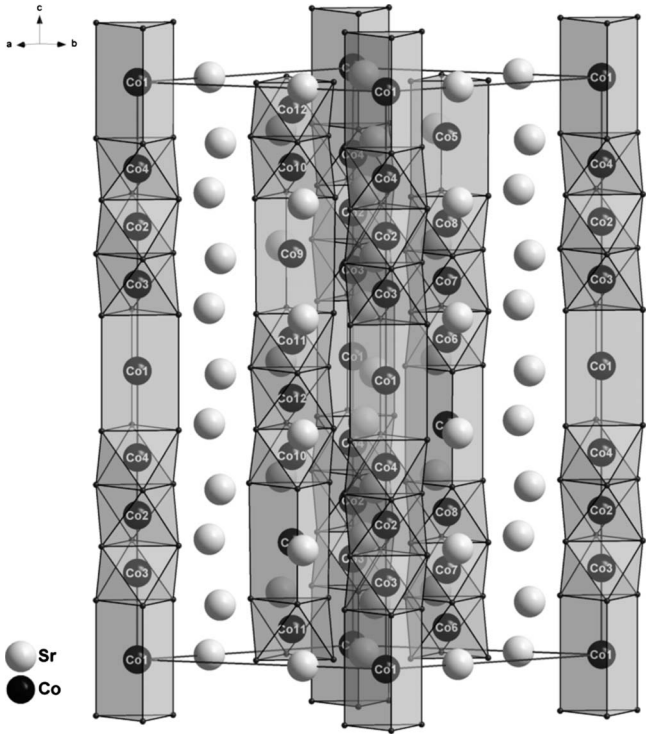

Figure 2. The structure of the homologous series of compounds, $A_{n+2}Co_nCo'O_{3n+3}$ (A=alkali earth elements), with n=3 (Wong-Ng *et al.*, 2010; Boulahya *et al.*, 1999a; Boulahya *et al.*, 1999b).

009-0961, 01-086-0614, and 01-075-4870 to 4873) (ICDD, 2010). Since X-ray reference powder diffraction patterns are critical for phase characterization, the second goal of this paper is to report the experimental powder patterns for these two phases for an inclusion in the PDF.

II. EXPERIMENTAL

A. Sample preparation

Samples were prepared from stoichiometric amounts of $CaCO_3$, Co_3O_4, and $SrCO_3$ using solid state high-temperature techniques. The starting samples were mixed,

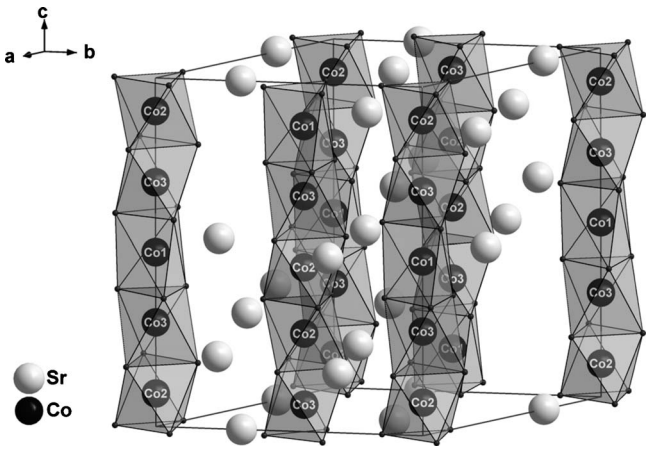

Figure 3. The structure of the homologous series of compounds, $A_{n+2}Co_nCo'O_{3n+3}$ (A=alkali earth elements), with n=4 (Wong-Ng *et al.*, 2010; Boulahya *et al.*, 1999a; Boulahya *et al.*, 1999b).

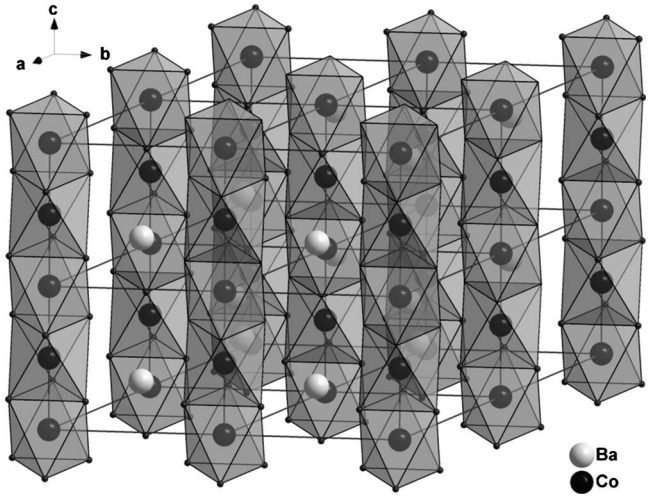

Figure 4. The structure of the homologous series of compounds, $A_{n+2}Co_nCo'O_{3n+3}$ (A=alkali earth elements), with $n=\infty$ (Wong-Ng *et al.*, 2010; Boulahya *et al.*, 1999a; Boulahya *et al.*, 1999b).

pelletized, and annealed at 750 °C for 1 day and subsequently annealed at 850 °C with intermediate grindings and pelletizations for another 7 days. The annealing process was repeated until no further changes were detected in the powder X-ray diffraction patterns.

B. X-ray powder diffraction

1. Phase identification

Powder X-ray diffraction was used to investigate the phase purity and establish the phase relationships. These experiments were carried out using a Phillips X-ray powder diffractometer with Cu $K\alpha$ radiation which was equipped with a series of Soller slits and a scintillation counter. The 2θ scanning range was from 10° to 80° and the step interval was

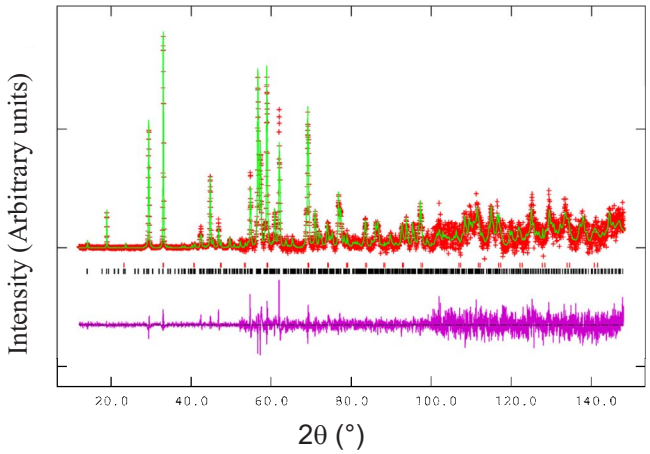

Figure 5. (Color online) Observed (crosses) and calculated (solid line) XRD intensity pattern for $(Sr_{0.8}Ca_{0.2})_5Co_4O_{12}$ at 300 K. The row of tick marks indicate the calculated peak positions. The difference pattern is plotted at same scale as the other patterns up to 50°2θ. At between 50 and 100°2θ, the scale has been magnified five times. At 2θ values higher than 100°, the scale has been magnified ten times. An impurity phase of $SrCoO_3$ was determined to be 3.9(2) mass %.

https://doi.org/10.1154/1.3555294 Published online by Cambridge University Press

TABLE III. Bond distances in $(Sr,Ca)_5Co_4O_{12}$. V_b represents bond valence sum (Brese and O'Keeffe, 1991; Brown and Altermatt, 1985). The V_b values for the mixed (Sr, Ca) sites were computed based on the respective site occupancy.

Atom 1	Atom 2	Site occupancy	Distance	V_b
Sr1/Ca1	O1	0.75/0.25	2.78 (2)	2.373
Sr1/Ca1	O1		2.58 (3)	
Sr1/Ca1	O2		2.60 (3)	
Sr1/Ca1	O3		2.71 (3)	
Sr1/Ca1	O4		2.38 (2)	
Sr1/Ca1	O5		2.51 (3)	
Sr1/Ca1	O11		2.33 (2)	
Sr1/Ca1	O12		2.62 (3)	
Sr2/Ca2	O1	0.85/0.15	2.47 (3)	2.085
Sr2/Ca2	O3		2.97 (2)	
Sr2/Ca2	O3		2.76 (2)	
Sr2/Ca2	O4		2.81 (3)	
Sr2/Ca2	O4		2.51 (3)	
Sr2/Ca2	O5		2.66 (2)	
Sr2/Ca2	O5		2.64 (2)	
Sr2/Ca2	O6		2.46 (2)	
Sr2/Ca2	O7		2.79 (2)	
Sr3/Ca3	O4	0.86/0.14	2.50 (2)	2.296
Sr3/Ca3	O5		2.68 (2)	
Sr3/Ca3	O6		2.74 (2)	
Sr3/Ca3	O6		2.60 (2)	
Sr3/Ca3	O7		2.53 (2)	
Sr3/Ca3	O7		2.66 (2)	
Sr3/Ca3	O8		2.58 (2)	
Sr3/Ca3	O9		2.414 (14)	
Sr3/Ca3	O10		3.07 (2)	
Sr4/Ca4	O6	0.86/0.14	2.70 (2)	2.264
Sr4/Ca4	O7		2.48 (2)	
Sr4/Ca4	O8		2.593 (14)	
Sr4/Ca4	O8		2.722 (14)	
Sr4/Ca4	O9		3.18 (2)	
Sr4/Ca4	O9		2.32 (2)	
Sr4/Ca4	O10		2.848 (14)	
Sr4/Ca4	O10		3.05 (2)	
Sr4/Ca4	O11		3.07 (2)	
Sr4/Ca4	O12		2.46 (2)	
Sr5/Ca5	O1	0.78/0.22	2.62 (2)	2.405
Sr5/Ca5	O2		2.38 (2)	
Sr5/Ca5	O8		2.50 (2)	
Sr5/Ca5	O9		3.21 (3)	
Sr5/Ca5	O10		2.39 (2)	
Sr5/Ca5	O11		2.69 (2)	
Sr5/Ca5	O11		2.652 (5)	
Sr5/Ca5	O12		2.550 (3)	
Sr5/Ca5	O12		2.73 (2)	
Co1	O3		1.976 (8)×3	2.758
Co1	O11		1.983(8)×3	
Co2	O6		1.889(8)×3	3.606
Co2	O8		1.904(8)×3	
Co3	O3		1.874(8)×3	3.571
Co3	O6		1.928(7)×3	
Co4	O8		1.913(8)×3	3.568
Co4	O11		1.888(8)×3	
Co5	O2		1.982(8)×3	2.888
	O10		1.975(8)×3	
Co6	O2		1.888(8)×3	3.417
	O5		1.913(7)×3	
Co7	O5		1.905(7)×3	3.714
	O7		1.867(7)×3	
Co8	O7		1.936(8)×3	3.530
Co8	O10		1.875(9)×3	
Co9	O4		1.929(8)×3	3.145
Co9	O9		1.933(8)×3	
Co10	O9		1.880(8)×3	3.479
Co10	O12		1.942(7)×3	
Co11	O1		1.938(7)×3	3.456
Co11	O4		1.888(8)×3	
Co12	O1		1.911(8)×3	3.433
Co12	O12		1.916(8)×3	
Co1	Co3		2.61 (2)	
Co1	Co4		2.58 (2)	
Co2	Co3		2.38 (2)	
Co2	Co4		2.41 (2)	
Co5	Co6		2.58 (2)	
Co5	Co8		2.60 (2)	
Co6	Co7		2.42 (2)	
Co7	Co8		2.40 (2)	
Co9	Co10		2.57 (2)	
Co9	Co11		2.58 (2)	
Co10	Co12		2.43 (2)	
Co11	Co12		2.41 (2)	

0.03°. The ICDD PDF reference diffraction patterns of the Ca-Sr-Co-O systems were used for performing phase identification.

2. Crystal structure analysis

The Ca-Sr-Co-O powders were mounted as acetone slurries in silicon zero-background holders. A PANalytical X'Pert Pro MPD diffractometer equipped with a PIXcel position-sensitive detector and a graphite diffracted beam monochromator was used to measure the powder patterns (Cu $K\alpha$ radiation, 40 kV, and 40 mA) from 5 to 148°2θ in 0.013° steps, counting for 0.5 s/step. All data processing and structural refinements were carried out using the Rietveld refinement technique with the GSAS software suite (Larson and von Dreele, 1992; Rietveld, 1969). Included in the refinements were the atomic coordinates and isotropic displacement coefficients, a scale factor, a sample displacement coefficient, and the unit-cell parameters. The peak profiles were described using a pseudo-Voigt function; for $(Sr_{0.8}Ca_{0.2})_5Co_4O_{11}$ the size broadening *ptec* and the anisotropic strain broadening terms S_{xy} were refined, and for $Sr_6Co_5O_{15}$ the profile Y strain term was refined. The backgrounds of the profiles were described using a six- or nine-term shifted Chebyshev polynomial. To ensure the correctness of structure, a VASP spin-polarized magnetic geometry optimization technique (with fixed lattice parameters) using "normal" precision and a plane wave cutoff energy of 400 eV was performed for optimization of geometry (Kresse and Furthmüller, 1996a, 1996b; Kresse and Joubert, 1999). GGA-PBE/PAW potentials were used with a $2\times2\times1$ k-point mesh for a spacing of $0.385\times0.385\times0.314$ Å^{-1}.

X-ray reference patterns were obtained with a Rietveld pattern decomposition technique (Larson and von Dreele,

https://doi.org/10.1154/1.3555294 Published online by Cambridge University Press

1992). Using this technique, the reported peak positions are calculated from the lattice parameters. For overlapped peaks, the intensities are summed, and an intensity-weighted d spacing is reported. Therefore, these patterns represent ideal specimen patterns. They are corrected for systematic errors both in d-spacing and intensity.

C. Bond valence sums (V_b) calculations

The bond valence sum values, V_b, of an atom i are defined as the sum of the bond valences v_{ij} of all the bonds from atoms i to atoms j. The most commonly adopted empirical expression for v_{ij} as a function of the interatomic distance d_{ij} is $v_{ij}=\exp[(R_0-d_{ij})/B]$. The parameter, B, is commonly taken to be a "universal" constant equal to 0.37 Å. V_b's for Sr/Ca and Co are calculated using the Brown-Altermatt empirical expression (Brese and O'Keeffe, 1991; Brown and Altermatt, 1985). The values of the reference distance R_0 for Sr-O and Ca-O are 2.118 and 2.065 Å, respectively (Brese and O'Keeffe, 1991; Brown and Altermatt, 1985). The V_b values for the mixed (Sr, Ca) sites were computed based on the respective site occupancy. The R_0 values for Co^{2+} and Co^{3+} have been reported to be 1.692 and 1.70 by Brese and O'Keeffe (1991), and the approximate value for Co^{4+} (1.708) has been estimated by extrapolation from the Co^{2+} and Co^{3+} values.

III. RESULTS AND DISCUSSION

The structures of the general $A_{n+2}B'B_nO_{3n+3}$ (A=Sr and Ca; B=Co) homologous series and of two representative members of the series, $(Sr_{0.8}Ca_{0.2})_5Co_4O_{12}$ and $Sr_6Co_5O_{15}$, and their reference X-ray powder diffraction patterns are described in the following.

A. General structure description of $A_{n+2}B'B_nO_{3n+3}$ (A=Sr and Ca; B=Co)

In the formula $A_{n+2}B_nB'O_{3n+3}$, A is an alkaline-earth element, B describes the cobalt ion inside the octahedral cage, and B' describes the cobalt ion inside a trigonal prism. $Sr_{n+2}Co_nCoO_{3n+3}$ consists of one-dimensional linear parallel $Co_2O_6^{6-}$ chains, built by successive alternating face-sharing CoO_6 trigonal prisms and CoO_6 octahedra along the hexagonal c axis (Wong-Ng *et al.*, 2010; Boulahya *et al.*, 1999a, 1999b; Stitzer *et al.*, 2001). This face-sharing feature is in contrast with $Ca_3Co_4O_9$ and $NaCo_2O_4$, which consists of edge-sharing CoO_6 octahedra (Masset *et al.*, 2000). The $Co_2O_6^{6-}$ chains can be considered as stacking of n number of octahedra alternating with one trigonal prism. The compounds of $A_{n+2}Co_nCo'O_{3n+3}$ can also be considered as ordered intergrowth between the $n=\infty$ ($ACoO_3$) and $n=1$ ($A_3Co_2O_6$) end members. These compounds are of interest to the thermoelectric community because it is thought that scattering of heat phonons is perpendicular to the structural Co-O chain directions, which lowers the thermal conductivity.

The structure of the homologous series of compounds, $A_{n+2}Co_nCo'O_{3n+3}$ (A=alkali earth elements), with n=1, 3, 4, and ∞, is shown from Figures 1–4 (Wong-Ng *et al.*, 2010; Boulahya *et al.*, 1999a, 1999b). Based on our previous study of phase equilibria of the SrO-CaO-CoO_x system, Ca substitutes in the Sr site for the n=3 and 4 members of the $Sr_{n+2}Co_nCo'O_{3n+3}$ series to the extent of $(Sr_{0.67}Ca_{0.33})_5Co_4O_{11}$ and $(Sr_{0.725}Ca_{0.275})_6Co_5O_x$, respectively (Wong-Ng *et al.*, 2010). The stability of these compounds is related to the size of the alkaline earth. For example, for A=Ca, only n=1 member can be prepared. When A=Sr, n=2, 3, and 4 can be prepared but not with n=1 member under the current processing conditions. For compounds with $n>4$, only the A=Ba analogs can be made.

TABLE IV. Rietveld refinement results of $Sr_6Co_5O_{15}$, $R32$.

R_{wp}	0.0593
R_p	0.0370
χ^2	7.178
Percentage from restraints	2.5
No. of observations	10 492
No. of variables	36
$R(F)$	0.0524
$R(F^2)$	0.0720
Normal probability plot, slope	1.6797
Intercept	−0.0044
ΔF, eÅ^{-3}, +	2.1 (near Co2)
⋯	−1.4

B. Structure of $(Sr_{0.8}Ca_{0.2})_5Co_4O_{12}$

Figure 5 gives the observed (crosses) and calculated (solid line) XRD intensity pattern for $(Sr_{0.8}Ca_{0.2})_5Co_4O_{12}$ at 300 K. Tables I–III give the Rietveld refinement results, the atomic coordinates, and the bond distances of $(Sr,Ca)_5Co_4O_{12}$, respectively. The oxygen coordinates that we report are those resulted from the VASP spin-polarized magnetic geometry optimization calculations, as they are more reliable than those from Rietveld refinements.

Based on the refinement results, the space group of $(Sr_{0.8}Ca_{0.2})_5Co_4O_{12}$ was determined to be $P3c1$ instead of

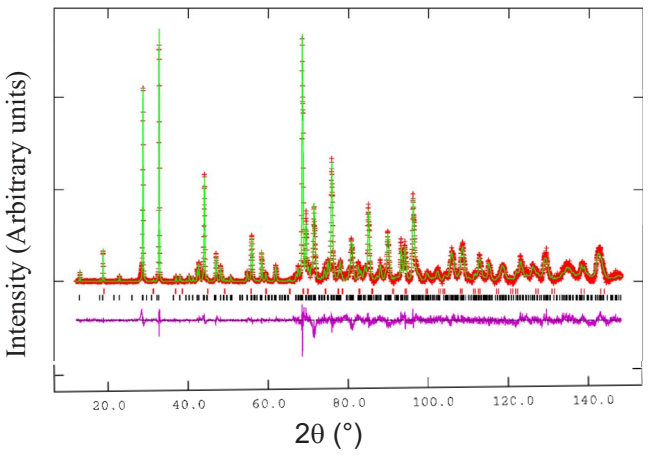

Figure 6. (Color online) Observed (crosses) and calculated (solid line) XRD intensity pattern for $Sr_6Co_5O_{15}$ at 300 K. The row of tick marks indicate the calculated peak positions. The difference pattern is plotted at same scale as the other patterns up to 65°2θ. At higher angles, the scale has been magnified five times. An impurity phase of Co_3O_4 was determined to be 2.1(1) mass fraction %.

https://doi.org/10.1154/1.3555294 Published online by Cambridge University Press

TABLE V. Atomic coordinates of atoms in $Sr_6Co_5O_{15}$.

Atom	x	y	z	Occupancy	U_{iso}	Site
Sr1	0.323 65(34)	0.0	0.0	1.0	0.021 82(27)	9*d*
Sr2	0.643 30(27)	0.0	$\frac{1}{2}$	1.0	0.021 82(27)	9*c*
Co1	0.0	0.0	$\frac{1}{2}$	1.0	0.0123(4)	3*b*
Co2	0.0	0.0	0.0976(5)	1.0	0.0123(4)	6*c*
Co3	0.0	0.0	0.295 59(33)	1.0	0.0123(4)	6*c*
O1	0.8376(14)	0.0	0.0	1.0	0.0182(13)	9*d*
O2	0.4933(10)	0.6849(12)	0.4776(6)	1.0	0.0182(13)	18*f*
O3	0.8402(9)	−0.0209(12)	0.6149(6)	1.0	0.0182(13)	18*f*

*P*321. The lattice parameters are $a=9.4196(2)$ Å, $c=19.9857(6)$ Å, $V=825.83$ Å^3, and $D_x=5.358$ g/cm^3. Ca was confirmed to substitute in the Sr site.

The structure of the $n=3$ member of $(Sr,Ca)_{n+2}Co_nCo'O_{3n+3}$ consists of linear chains of three units of octahedra alternating with one unit of trigonal prism, giving rise to a total of nine octahedra and three trigonal prisms per chain along the *c* axis within the unit cell (Figure 2). The Co ions in the columns face each other at distances between 2.419(12) and 2.534(4) Å. This relatively short distance will likely produce a large electrostatic repulsion between the metal ions. The oxygen ions of face-shared triangles screen the Coulomb interaction between Co ions and therefore weaken the repulsion. As the distances between the Co ions in the prisms and in the octahedra are only about 2.5 Å, whereas the distances between Co ions in the parallel chains are about 5 Å, there are possible interactions between Co ions in the same chains via superexchange, but these interactions are not likely to occur between the neighboring chains.

At present, there is no conclusive evidence about whether there is charge ordering of Co ions along the chain of $A_{n+2}Co_nCo'O_{3n+3}$ (A=alkaline-earth cations). According to Maignan *et al.* (2003), in $Ca_3Co_2O_6$ ($n=1$ member), no evidence of Co^{2+}/Co^{4+} ordering (Co^{2+} ions occupy the prismatic position, while Co^{4+} occupies the octahedral sites) was detected from high-temperature magnetic susceptibility measurements (Maignan *et al.*, 2000). The cobalt species are trivalent, and the larger cation (high-spin Co^{3+}) occupies the trigonal prism site, while the low-spin Co^{3+} occupies the octahedral site. Fjellvåg *et al.* (1996) found the bond valence V_b value for the prismatic Co site to be 2.25 while the octahedral Co site to have a much higher valence of 3.35. Therefore, there could be charge ordering of Co^{2+}/Co^{4+} or ordering of low- and high-spin Co^{3+} species.

The average valence for the Co ions in $(Sr_{0.8}Ca_{0.2})_5Co_4O_{12}$ was calculated to be 3.5. In $(Sr_{0.8}Ca_{0.2})_5Co_4O_{12}$, if we assume the valence of the three octahedral Co sites to be 4+ and the valence of the Co in the trigonal prism to be 2+, then the charge balanced formula can be written as $(Sr,Ca)^{2+}{}_5Co^{4+}{}_3Co^{2+}O_{12}{}^{2-}$. As indicated in Table I, the Co sites that are inside the trigonal prisms are labeled as Co1, Co5, and Co9. The values of V_b at these trigonal prism sites, while smaller than those of the octahedral sites, are greater than the ideal value of 2.0 (2.758 for Co1, 2.888 for Co5, and 3.145 for Co9) possibly due to the presence of compressive stress (or the size of the cage too small). At the same time the V_b values of the octahedral Co sites are all less than the ideal value of 4+ (ranging from 3.433 to 3.714), indicating tensile stress or underbonding because the sizes of the cages where these cations reside are too large. It is also possible that all these Co sites have mixed-valence characters because of metal to metal (Co/Co) interactions along the chains.

The Sr^{2+}/Ca^{2+} ions have three different types of cage environment or coordination number, namely, one eight-coordination cage (Sr1/Ca1, with average Sr/Ca-O distance of 2.56 Å), three nine-coordination cages (average distances of 2.68 Å for Sr2/Ca2, 2.64 Å for Sr3/Ca3, and 2.64 Å for Sr5/Ca5), and one ten-coordination cage (average distance of 2.74 Å for Sr4/Ca4). The V_b values of these sites are all greater than 2.0 (Table III), indicating compressive stress or overbonding.

C. Structure of $Sr_6Co_5O_{15}$

Our refinement results show the structure of $Sr_6Co_5O_{15}$ to be *R*32. The crystal structure of $Sr_6Co_5O_{15}$ is shown in Figure 3. Table IV and Figure 6 give the Rietveld refinement

TABLE VI. Bond distances of atoms in $Sr_6Co_5O_{15}$. V_b represents bond valence sum values (Brese and O'Keeffe, 1991; Brown and Altermatt, 1985).

Atom	Atom	Distance	(Å)	V_b
Sr1	O1	2.662(3)	×2	2.093
Sr1	O2	2.533(8)	×2	
Sr1	O2	2.865(8)	×2	
Sr1	O3	3.063(10)	×2	
Sr1	O3	2.661(10)	×2	
Sr2	O1	2.568(8)	×2	2.475
Sr2	O2	2.608(10)	×2	
Sr2	O2	2.726(10)	×2	
Sr2	O3	2.437(8)	×2	
Sr2	O3	3.163(6)	×2	
Co1	Co3	2.534(4)		
Co1	Co3	2.534(4)		
Co2	Co2	2.419(12)		
Co2	Co3	2.454(9)		
Co3	Co1	2.534(4)		
Co4	Co2	2.454(9)		
Co1	O3	2.018(6)	×6	2.540
Co2	O1	1.960(10)	×3	3.580
Co2	O2	1.833(8)	×3	
Co3	O2	1.954(8)	×3	3.744
Co3	O3	1.809(8)	×3	

https://doi.org/10.1154/1.3555294 Published online by Cambridge University Press

TABLE VII. X-ray reference pattern for $(Ca_{0.2}Sr_{0.8})_5Co_4O_{11}$, $P3c1$ (No. 165), a=9.4196(2) Å, c=19.9857(6) Å, V=825.83 Å^3, and D_x=5.358 g/cm^3. The symbol d_{cal} refers to calculated d-spacing values, I_{obs} refers to observed integrated intensity value (scaled according to the maximum value of 999; the symbol * indicates the strongest peak), the hkl values are the Miller indexes, and M and + refer to peaks containing contributions from two and more than two reflections, respectively.

d_{cal} (Å)	I_{obs}	h	k	l	d_{cal} (Å)	I_{obs}	h	k	l	d_{cal} (Å)	I_{obs}	h	k	l
6.3193	29	1	0	2	4.7098	118	1	1	0	3.7764	10	2	0	−2
3.3309	7	0	0	6	3.1597	8	2	0	4	3.0476	736	1	1	5
3.0473	8	2	1	1	2.9462	5	2	1	2+	2.7981	22	2	1	3M
2.7981	22	2	1	−3M	2.7192	999*	3	0	0	2.5800	6	2	0	−6
2.3887	10	1	0	−8	2.3549	12	2	2	0	2.3387	5	2	2	1
2.2482	22	3	1	1M	2.2482	22	3	1	−1M	2.2203	8	2	2	3
2.2067	15	3	1	−2	2.1423	73	3	1	3+	2.1304	120	2	0	8
2.0949	14	2	1	7+	2.0611	11	3	1	−4+	2.0290	526	2	2	5
1.9985	66	0	0	10M	1.9985	66	4	0	2M	1.9410	199	2	1	−8+
1.8398	79	1	1	10	1.8395	13	3	2	2	1.8017	21	3	2	−3
1.7801	5	4	1	0	1.7732	6	3	1	−7	1.6770	69	3	1	8
1.6316	5	3	2	6	1.6262	170	4	1	5+	1.6104	129	3	0	10+
1.5798	14	4	0	−8	1.5700	159	3	3	0	1.5238	48	2	2	10
1.5020	12	4	2	3	1.4979	126	3	2	−8	1.4310	6	5	1	−3
1.3660	31	5	0	8	1.3596	137	6	0	0	1.3565	10	4	2	−7+
1.3293	40	4	1	10+	1.3120	15	4	2	8	1.3063	5	5	2	0
1.2821	44	1	1	15	1.2716	11	3	1	13	1.2638	13	5	1	−8
1.2417	60	5	2	5+	1.2346	56	3	3	10+	1.2229	9	6	1	3
1.1944	12	2	0	−16	1.1816	5	4	3	−8	1.1596	28	2	2	15
1.1576	17	2	1	16M	1.1576	17	5	3	−2M	1.1405	6	6	1	−7
1.1295	31	4	4	5	1.1241	33	6	0	10+	1.0934	16	5	2	−10+
1.0667	42	4	1	15+	1.0561	44	5	3	8	1.0431	29	7	1	5+
1.0390	13	3	2	16	1.0319	9	5	4	−3	1.0305	22	6	2	−8
1.0278	57	6	3	0	1.0145	13	4	4	10	0.9993	5	0	0	20
0.9918	12	5	0	−16	0.9857	7	7	2	3	0.9775	6	1	1	20
0.9705	6	4	2	−16	0.9671	5	6	1	13	0.9637	10	5	4	−8
0.9505	24	5	1	16+	0.9441	18	8	0	8	0.9380	25	3	0	−20+
0.9328	30	5	2	−15+	0.9169	8	5	5	5	0.9140	23	6	3	10+
0.9064	20	9	0	0	0.8919	15	8	1	−8	0.8823	12	4	4	15
0.8815	6	6	1	−16	0.8714	9	4	1	20+	0.8688	36	8	2	−5+
0.8640	13	5	4	−13	0.8521	23	5	3	−16	0.8482	14	9	1	3
0.8430	23	3	3	20	0.8392	26	7	1	15+	0.8385	19	6	2	16
0.8363	8	7	2	13	0.8284	7	6	1	18	0.8276	11	7	4	−5+
0.8255	22	8	3	−2+	0.8192	7	9	1	−7	0.8131	10	8	2	10+
0.8091	42	6	5	−8	0.8052	33	6	0	20+	0.8038	22	8	3	−6+

results. In Figure 6, the observed (crosses) and calculated (solid line) XRD intensity pattern for $Sr_6Co_5O_{15}$ at 295 K are shown. The difference pattern is plotted at the same scale as the other patterns. Tables V and VI provide the atomic coordinates and bond distances of $Sr_6Co_5O_{15}$. Similar to $(Sr_{0.8}Ca_{0.2})_5Co_4O_{12}$, the oxygen coordinates that we report are those resulted from the VASP spin-polarized magnetic geometry optimization calculations.

All Co ions in $Sr_6Co_5O_{15}$ are six coordinated. Co1 has a trigonal prism environment with all six Co-O distances equal at 2.018(6) Å. Both Co2 and Co3 have a distorted octahedral environment with bond distances ranging from 1.809(8) to 1.960(10) Å. Similar to the structure of $(Sr_{0.8}Ca_{0.2})_5Co_4O_{12}$, the V_b values of Co in the trigonal prisms tend to be lower (close to the value of 2.5) than those in the octahedra (3.580 and 3.744). The average oxidation state of Co in $Sr_6Co_5O_{15}$ is 3.6. One can achieve charge balance if all the Co's in the octahedral sites of $Sr_6Co_5O_{15}$ have a valence of 4+, and the one Co in the trigonal prism site has a valence of 2+, leading to the formula $Sr_6^{2+}Co_4^{4+}Co^{2+}O_{15}$. The 2.5 value of V_b at the trigonal prism Co1 site is possibly due to the presence of compressive stress as compared to the ideal valence state of 2+. In the octahedral Co2 and Co3 sites, both V_b values are less than 4+, indicating tensile stress. Similar to $(Sr_{0.8}Ca_{0.2})_5Co_4O_{12}$, the Co…Co distances which range from 2.38(2) to 2.61(2) Å are much shorter than those between chains (about 5 Å); therefore, superexchange between Co ions would not be likely among chains.

Two crystallographically independent Sr environments were found; both are coordinated to ten oxygen atoms (average Sr1-O and Sr2-O distances of 2.09 and 2.48 Å, respectively). By comparing these coordination environments with the $(Sr_{0.8}Ca_{0.2})_5Co_4O_{12}$ structure [containing eight-, nine-, and tenfold (Sr, Ca)-O coordinations], we found that the alkaline-earth oxide cages in $Sr_6Co_5O_{15}$ have a relatively larger average cage size. Therefore, as n increases in $Sr_{n+2}Co'Co_nO_{3n+3}$, the average alkaline-earth cage size increases accordingly. It is clear from our results and those of

https://doi.org/10.1154/1.3555294 Published online by Cambridge University Press

TABLE VIII. X-ray reference pattern for $Sr_6Co_5O_{12}$, $R32$ (No. 155), a=9.497 64(12) Å, c=12.3956(2) Å, V=968.34 Å^3, and D_x=5.455 g/cm^3. The symbol d_{cal} refers to calculated d-spacing values, I_{obs} refers to observed integrated intensity value (scaled according to the maximum value of 999; the symbol * indicates the strongest peak), the hkl values are the Miller indexes, and M and + refer to peaks containing contributions from two and more than two reflections, respectively.

d_{cal} (Å)	I_{obs}	h	k	l	d_{cal} (Å)	I_{obs}	h	k	l	d_{cal} (Å)	I_{obs}	h	k	l
6.8536	27	1	0	1	4.7488	88	1	1	0	3.9034	15	2	0	−1
3.1171	959	1	1	3	2.7417	999*	3	0	0	2.3741	16	2	2	0M
2.3741	16	1	0	−5M	2.2436	30	3	1	−1	2.1948	17	2	1	4
2.1408	62	3	1	2	2.1232	9120	2	0	5	2.066	130	0	0	6
2.0587	592	2	2	3	2.0286	10	4	0	1	1.9383	180	2	1	−5
1.8944	103	1	1	6	1.8655	13	3	2	1	1.8372	5	3	1	−4
1.8052	28	3	2	−2	1.6787	73	3	1	5	1.6500	183	3	0	+6
1.6463	203	4	1	−3+	1.6307	6	5	0	−1	1.6117	5	3	2	4
1.5829	193	3	3	0M	1.5829	193	4	0	−5M	1.5586	64	2	2	6
1.5077	11	4	2	2	1.5015	128	3	2	−5	1.4370	9	5	1	−2
1.3988	8	3	1	−7	1.3894	11	4	2	−4	1.3709	194	6	0	0M
1.3709	194	5	0	5M	1.3549	61	4	1	−6+	1.3442	8	4	3	1
1.3335	9	5	1	4	1.3228	69	1	1	9	1.3170	18	4	2	5
1.2818	13	3	1	8	1.2691	18	5	1	−5	1.2565	54	3	3	6
1.2549	77	5	2	3+	1.2480	9	6	1	−1	1.2294	8	6	1	2
1.2257	23	1	0	10	1.1975	9	3	2	−8	1.1914	45	2	2	9
1.1869	19	4	3	−5M	1.1869	19	2	0	−10M	1.1698	13	5	3	−1
1.1627	11	6	1	−4	1.1514	14	2	1	10	1.1423	48	6	0	6+
1.1410	44	4	4	3	1.1106	24	5	2	6+	1.0927	60	4	1	9+
1.0892	8	3	1	−10	1.0618	43	5	3	5	1.0535	42	7	1	−3+
1.0383	11	5	4	−2	1.0362	100	6	3	0+	1.0330	8	0	0	12
1.0294	14	4	4	6	1.0246	5	8	0	−1	1.0094	11	1	1	12
0.9971	5	5	4	4	0.9919	8	7	2	2	0.9900	13	5	0	−10
0.9791	8	5	3	−7	0.9749	5	6	1	8	0.9692	21	5	4	−5M
0.9692	21	4	2	−10M	0.9666	40	3	0	−12+	0.9637	13	7	1	−6+
0.9559	5	7	2	−4	0.9519	41	5	2	−9+	0.9496	33	8	0	5M
0.9496	33	5	1	10M	0.9472	8	2	2	12	0.9408	5	6	4	−1
0.9313	6	7	2	5	0.9263	33	6	3	−6+	0.9256	11	5	5	3
0.9139	29	9	0	0M	0.9138	29	4	3	10M	0.8992	14	4	4	9
0.8974	13	8	1	−5	0.8953	12	4	1	12+	0.8817	11	6	1	−10
0.8770	43	8	2	3+	0.8710	16	5	4	−8	0.8651	31	3	3	12
0.8629	6	5	5	6	0.8602	6	9	1	−1	0.8544	32	7	1	9+
0.8540	12	9	1	2	0.8528	25	5	3	−10+	0.8431	5	7	2	8
0.8394	18	6	2	10	0.8383	8	6	1	11	0.8358	17	9	0	6+
0.8353	20	7	4	3+	0.8333	13	8	3	−1	0.8307	10	9	1	−4
0.8250	29	6	0	−12+	0.8231	15	8	2	6+	0.8143	93	1	1	15+
0.8133	12	7	0	−11+	0.8128	16	5	2	−12+	0.8036	6	9	2	−2

the Ca- and Ba-homologous series (Boulahya *et al.*, 1999b; Fjellvåg *et al.*, 1996) that the size of the alkaline-earth cage is important for the stability of the homologous members; the higher the n value is, the larger the cage size is. For example, the coordination number for Ca^{2+} is 8 in $Ca_3Co_2O_6$ (n =1 phase) (Fjellvåg *et al.*, 1996) but is greater than 10 around the Ba^{2+} in $Ba_8Co_7O_{21}$ (n=6 member) (Taguchi *et al.*, 1977). The alkaline-earth ions also play a role of adjusting the spacing between chains.

D. Reference X-ray powder diffraction patterns

The reference X-ray powder diffraction patterns for the phases $(Sr,Ca)_5Co_4O_{11}$ and $Sr_6Co_5O_{15}$ have been prepared and submitted to the ICDD to be included in the Powder Diffraction File. Tables VII and VIII give the reference patterns for $(Sr,Ca)_5Co_4O_{11}$ and $Sr_6Co_5O_{15}$, respectively. In these tables, the symbols M and + refer to peaks containing contributions from two and more than two reflections, respectively. The symbol * indicates the particular peak has the strongest intensity of the entire pattern and is designated a value of "999." The intensity values reported are integrated intensities rather than peak heights.

IV. CONCLUSION

The structures of $(Sr,Ca)_5Co_4O_{11}$ and of $Sr_6Co_5O_{15}$ in the $(Sr,Ca)_{n+2}Co'Co_nO_{3n+3}$ system have been studied because of their potential applications as thermoelectric materials. These structures belong to the n=3 and n=4 members of the homologous series of $A_{n+2}Co_nCo'O_{3n+3}$ [A=Sr and (Sr, Ca)]. The salient feature of the structures is the linear chains consisting of alternating CoO_6 trigonal prisms with n

https://doi.org/10.1154/1.3555294 Published online by Cambridge University Press

members of CoO_6 octahedra. It is clear from our results and from studies of the Ca- and Ba-homologous series that the size of the alkaline-earth cage is important for the stability of the homologous members; the higher the n value is, the larger the alkaline-earth cage size is. The alkaline-earth ions also play a role of adjusting the spacing between chains. The possible charge ordering along the chain direction still needs to be further studied. The reference X-ray powder diffraction patterns of these two phases have been submitted to the Powder Diffraction File. As cobalt oxides are stable materials at high temperature that possess interesting thermoelectric properties, continuing research efforts in this class of materials in the future are of great interest.

ACKNOWLEDGMENT

The partial financial support from ICDD for the preparation of the reference X-ray powder diffraction patterns is acknowledged.

Abraham, F., Minaud, S., and Renard, C. (**1994**). "Preliminary crystal structure of mixed-valency $Sr_4Ni_3O_9$, the actual formula of the so-called $Sr_5Ni_4O_{11}$," J. Mater. Chem. **4**, 1763–1764.

Blake, G. R., Battle, P. D., Sloan, J., Vent, J. F., Darriet, J., and Weill, F. (**1999**). "Neutron diffraction study of the structures of $Ba_5CuIr_3O_{12}$ and $Ba_{16}Cu_3Ir_{10}O_{39}$," Chem. Mater. **11**, 1551–1558.

Boulahya, K., Parras, M., and González-Calbet, J. M. (**1999a**). "The $A_{n+2}B_nB'O_{3n+3}$ family (B=B'=Co): Ordered intergrowth between 2H-$BaCoO_3$ and $Ca_3Co_2O_6$ structures," J. Solid State Chem. **145**, 116–127.

Boulahya, K., Parras, M., and González-Calbet, J. M. (**1999b**). "Cation deficiency in (Ba,Sr)$Co_{1-x}O_y$ hexagonal perovskite related oxides: New members of the $A_{n+2}B'B_nO_{3n+3}$ homologous series," J. Solid State Chem. **142**, 419–427.

Brese, N. E. and O'Keeffe, M. (**1991**). "Bond-valence parameters for solids," Acta Crystallogr., Sect. B: Struct. Sci. **47**, 192–197.

Brown, I. D. and Altermatt, D. (**1985**). "Bond-valence parameters obtained from a systematic analysis of the inorganic crystal structure database," Acta Crystallogr., Sect. B: Struct. Sci. **41**, 244–247.

Dresselhaus, M. S., Chen, G., Tang, M. Y., Yang, R. G., Lee, H., Wang, D. Z., Ren, Z. F., Fleurial, J. P., and Gogna, P. (**2007**). "Enhanced thermopower in PbSe nanocrystal quantum dot superlattices," Adv. Mater. **19**, 1043–1053.

Fjellvåg, H., Gulbrandsen, E., Aasland, S., Olsem, A., and Hauback, B. C. (**1996**). "Crystal structure and possible charge ordering in one-dimensional $Ca_3Co_2O_6$," J. Solid State Chem. **124**, 190–194.

Funahashi, R., Urata, S., and Kitawaki, M. (**2004**). "Exploration of n-type oxides by high throughput screening," Appl. Surf. Sci. **223**, 44–48.

Ghamaty, S. and Eisner, N. B. (**1999**). "Development of quantum well thermoelectric films," Proceedings of the 18th International Conference on Thermoelectrics, Baltimore, MD, pp. 485–488.

Grebille, D., Lambert, S., Bouree, F., and Petricek, V. (**2004**). "Contribution of powder diffraction for structure refinements of aperiodic misfit cobalt oxides," J. Appl. Crystallogr. **37**, 823–831.

Harrison, W. T. A., Hegwood, S. L., and Jacobson, A. L. (**1995**). "A powder neutron diffraction determination of the structure of $Sr_6Co_5O_{15}$, formerly described as the low-temperature hexagonal form of $SrCoO_{3-x}$," J. Chem. Soc., Chem. Commun. 1953–1954.

Hernando, M., Boulahya, K., Parras, M., González-Calbet, J. M., and Amador, U. (**2003**). "Synthesis and microstructural characterization of two new one-dimensional members of the $(A_3NiMnO_6)_\alpha(A_3Mn_3O_9)_\beta$ homologous series (A=Ba,Sr)," Eur. J. Inorg. Chem. 2419–2425.

Hsu, K. F., Loo, S., Guo, F., Chen, W., Dyck, J. S., Uher, C., Hogan, T., Polychroniadis, E. K., and Kanatzidis, M. G. (**2004**). "Cubic $AgPb_mSbTe_{2+m}$: Bulk thermoelectric materials with high figure of merit," ChemInform **35** (17).

ICDD (**2010**). "Powder Diffraction File," edited by S. Kabekkodu, International Centre for Diffraction Data, Newtown Square, Pennsylvania.

Iwasaki, K., Ito, T., Matsui, T., Nagasaki, T., Ohta, S., and Koumoto, K. (**2006**). "Synthesis of an oxygen nonstoichiometric $Sr_6Co_5O_{15}$ phase," Mater. Res. Bull. **41**, 732–739.

Iwasaki, K., Yamane, H., Kubota, S., Takahashi, J., and Shimada, M. (**2003**). "Power factors of $Ca_3Co_2O_6$ and $Ca_3Co_2O_6$-based solid solutions," J. Alloys Compd. **358**, 210–215.

Kresse, G. and Furthmüller, J. (**1996a**). "Efficient iterative schemes for *ab initio* total-energy calculations using a plane-wave basis set," Phys. Rev. B **54**, 11169–11186.

Kresse, G. and Furthmüller, J. (**1996b**). "Efficiency of ab-initio total energy calculations for metals and semiconductors using a plane-wave basis set," Comput. Mater. Sci. **6**, 15–50.

Kresse, G. and Joubert, D. (**1999**). "From ultrasoft pseudopotentials to the projector augmented-wave method," Phys. Rev. B **59**, 1758–1775.

Larson, A. C. and von Dreele, R. B. (**1992**). "GSAS-General Structure Analysis system," U.S. Government contract (W-7405-ENG-36) by the Los Alamos National Laboratory, which is operated by the University of California for the U.S. Department of Energy.

Lee, J. and Holland, G. (**1991**). "Identification of a new strontium Ni(III) oxide prepared in molten hydroxide," J. Solid State Chem. **93**, 267–271.

Maignan, A., Hébert, S., Martin, C., and Flahaut, D. (**2003**). "One dimensional compounds with large thermoelectric power factor," Mater. Sci. Eng., B **104**, 1298–1299.

Maignan, A., Michel, C., Masset, A. C., Martin, C., and Raveau, B. (**2000**). "Single crystal study of the one dimensional $Ca_3Co_2O_6$ compound: Five stable configurations for the Ising triangular lattice," Eur. Phys. J. B **15**, 657–663.

Masset, A. C., Michel, C., Maignan, A., Hervieu, M., Toulemonde, O., Studer, F., and Raveau, B. (**2000**). "Misfit-layered cobaltite with an anisotropic giant magnetoresistance: $Ca_3Co_4O_9$," Phys. Rev. B **62**, 166–175.

Mikami, M. and Funahashi, R. (**2005**). "The effect of element substitution on high-temperature thermoelectric properties of $Ca_3Co_2O_6$ compounds," J. Solid State Chem. **178**, 1670–1674.

Mikami, M., Funashashi, R., Yoshimura, M., Mori, Y., and Sasaki, T. (**2003**). "High-temperature thermoelectric properties of single-crystal $Ca_3Co_2O_6$," J. Appl. Phys. **94**, 6579–6582.

Minami, H., Itaka, K., Kawaji, H., Wang, Q. J., Koinuma, H., and Lippmaa, M. (**2002**). "Rapid synthesis and characterization of $(Ca_{1-x}Ba_x)_3Co_4O_9$ thin films using combinatorial methods," Appl. Surf. Sci. **197–198**, 442–447.

Rietveld, H. M. (**1969**). "A profile refinement method for nuclear and magnetic structures," J. Appl. Crystallogr. **2**, 65–71.

Rodriguez, J., Gonzalez, C. J. M., Grenier, J. C., Pannetier, J., and Anne, M. (**1987**). "Phase transitions in $Sr_2Co_2O_5$: A neutron thermodiffracometry study," Solid State Commun. **62**, 231–234.

Stitzer, K. E., Darriet, J., and zur Loye, H.-C. (**2001**). "Advances in the synthesis and structural description of 2H-hexagonal perovskite-related oxides," Curr. Opin. Solid State Mater. Sci. **5**, 535–544.

Sun, J., Li, G., Li, Z., You, L., and Lin, J. (**2006**). "Crystal growth and structure determination of oxygen-deficient $Sr_6Co_5O_{15}$," Inorg. Chem. **45**, 8394–8402.

Taguchi, H., Takeda, Y., Kanamaru, F., Shimada, M., and Koizumi, M. (**1977**). "Barium cobalt trioxide," Acta Crystallogr., Sect. B: Struct. Sci. **33**, 1298–1299.

Terasaki, I., Sasago, Y., and Uchinokura, K. (**1997**). "Large thermoelectric power in $NaCo_2O_4$ single crystals," Phys. Rev. B **56**, R12685-R12687.

Tritt, T. M. (**1996**). "Thermoelectrics run hot and cold," Science **272**, 1276–1277.

Tritt, T. M. and Subramanian, M. A., guest editors (**2006**). "Thermoelectric materials, phenomena, and applications: A bird's eye view," MRS Bull. **31**, 188–195.

Venkatasubramanian, R., Siivola, E., Colpitts, T., and O'Quinn, B. (**2001**). "Growth of one-dimensional Si/SiGe heterostructures by thermal CVD," Nature (London) **413**, 597–602.

Wong-Ng, W., Liu, G., Martin, J., Thomas, E. L., Lowhorn, N., and Kaduk, J. A. (**2010**). "Phase compatibility and thermoelectric properties of compounds in the Sr-Ca-Co-O System," J. Appl. Phys. **107**, 033508.